Received: 4 October 2019 | Accepted: 13 December 2019

DOI: 10.1111/nrm.12254

Natural Resource Modeling WILEY

Observed and projected trends of extreme precipitation and maximum temperature during 1992–2100 in Isfahan province, Iran using REMO model and copula theory

Maryam Mirakbari[1] | **Tayyebeh Mesbahzadeh**[1] | **Farshad Soleimani Sardoo**[2,3] | **Mario M. Miglietta**[4] | **Nir Y. Krakauer**[5] | **Nahid Alipour**[3]

[1]Department of Reclamation of Arid and Mountain Regions, Faculty of Natural Resources, University of Tehran, Tehran, Iran

[2]Department of Nature Engineering, Faculty of Natural Resources, University of Jiroft, Jiroft, Iran

[3]Department of Reclamation of Arid and Mountain Regions, Faculty of Natural Resources, University of Tehran, Tehran, Iran

[4]Institute of Atmospheric Sciences and Climate of the Italian National Research Council (ISAC-CNR), Padova, Italy

[5]Department of Civil Engineering, The City College of New York, New York, New York

Correspondence
Tayyebeh Mesbahzadeh, Faculty of Natural Resources, University of Tehran, 77871-31587 Tehran, Iran.
Email: tmesbah@ut.ac.ir

Abstract

Meteorological extreme events have a major impact on water resources, economic development, and ecosystem health. In this study, maximum precipitation and maximum temperature indices were derived for Isfahan province, in central Iran, over the historical (1992–2017) and future (2020–2100) periods. Precipitation and maximum temperature data from the REMO model under RCP4.5 scenario were used to investigate changes in extreme values over the future period. The results showed that extreme precipitation in the historical and future periods has respectively a decreasing and increasing trend. Based on the extreme indices, temperature in the study area has a significant increasing trend in the baseline and future period. Various combinations of extreme precipitation indicators were created for joint modeling by copula theory. Copula modeling for the three weather stations for which REMO had satisfactory performance in simulating extremes over the historic period showed that the average return period of extreme precipitation combinations will be reduced in the future period compared to the historical period at Daran and Shahreza, while the

average return period of combinations will have both increasing and decreasing trends at Naeen.

Recommendations for Resource Managers

- Knowing information about the probability of occurrence of extreme precipitation with a certain value that exceeds a certain threshold will help planning for water resource systems under drought conditions and future increasing temperature.
- The joint return period of extreme precipitation can help to know the return period of extreme events such as floods and droughts.
- The findings of this study are important to assess the prediction of climate extreme. Also, these results can be useful to provide the appropriate strategies for water resources managers in drought conditions under future increasing temperature.

KEYWORDS
climate change, Copula, extreme precipitation and maximum temperature indices, REMO

1 | INTRODUCTION

Global warming is one of the most important issues in today's society, and has affected various aspects of human life. Studies have shown that warming over the last 50 years has been dominantly related to human activities (IPCC, 2013). Global warming manifests as an increase in mean temperature at different spatial scales, from local to regional, continental, hemispheric, and global (Kundzewicz & Huang, 2010; IPCC, 2013; R. Li & Geng, 2013). According to the Intergovernmental Panel on Climate Change (IPCC), the average global surface air temperature has increased by 0.85 K from 1880 to 2012 (IPCC, 2013). As the number of hot days and nights has increased globally, the frequency of heat waves has increased in many areas. Under global warming, climate change is manifested also by an increasing number of floods and droughts. The nature of climate change at regional scale is influenced by local physical-geographical characteristics and climate conditions. Generally, mountainous, continental, and Arctic regions are more sensitive to climate change, while coastal areas are less sensitive (Battisti & Naylor, 2009; IPCC, 1996).

Extreme events such as floods, droughts, and hot and cold waves may be more affected by climate change than averages, in that even a small change in the mean climate parameters may be associated with a large change in extreme event frequency and intensity (IPCC, 2012; Katz & Brown, 1992; Meehl, Zwiers, Evans, & Knutson, 2000). These extremes have a strong impact on natural ecosystems and human activities, such as agricultural production, urban planning, water resources management and human health (Easterling et al., 2000; IPCC, 2013; Ngo &

Horton, 2016; Vogt, Vogt, & Gmur, 2016; Wang, Gebremichael, & Yan, 2010). Changes in climate extreme events such as drought, floods, and heat waves are a disaster for human communities and environmental ecosystems (Easterling et al., 2000; Mann et al., 2017; Sisco, Bosetti, & Weber, 2017). According to the World Meteorological Organization (WMO, 2013), more than 3.7 million people died between 2001 and 2010 due to climate extremes. Changes in climate extreme events, such as high temperature and heavy rainfall, may alter the severity, frequency, and duration of climate phenomena (drought, floods, etc.), that can cause serious damage.

Identifying the severity, frequency, and duration of extreme events is crucial for providing strategies to counter their effects (Choi et al., 2009). Although interest in climate change studies has increased, there have been fewer studies investigating climate extreme events. Most studies have examined the variation of monthly, annual, and seasonal mean values of climate parameters (Almazroui, Nazrul Islam, Saeed, Alkhalaf, & Dambul, 2017; Alves et al., 2016; Gagnon, Singh, Rousselle, & Roy, 2005; Ludwing et al., 2019; Marengo et al., 2009; Palatella, Miglietta, Paradisi, & Lionello, 2010; Pandey, Das, Jhajharia, & Pandey, 2018; Pervez & Henebry, 2014; Silva & Mendes, 2015). To facilitate research on climate extremes and their trends, the Expert Team on Climate Change Detection and Indices (ETCCDI) of WMO and the World Climate Research Program (WCRP) have identified a set of 27 indicators describing the extreme character of climate events. These indices are derived from daily data on surface air temperature and precipitation (Donat et al., 2013; Frich et al., 2002).

General circulation models (GCMs) and regional climate models (RCMs) can be useful for projecting the future frequency, severity, and duration of extreme events. Many researchers have studied climate extreme indices using observational or climate model data (Frich et al., 2002; Klein Tank, & Können, 2003; Meehl & Claudia, 2004; Meehl et al., 2000; Sillmann & Roeckner, 2008; Tebaldi, Hayhoe, Arblaster, & Meehl, 2006). For example, Sillmann, Kharin, Zwiers, Zhang, and Bronaugh (2013) applied the Fifth Assessment Report (AR5) GCM simulations to analyze extreme precipitation indices globally. The results of this study showed general increases in heavy precipitation, except in Australia, Central America, South Africa, and the Mediterranean. Santos and Oliveira (2017) examined precipitation and extreme temperature in Brazil from 1970 to 2006 using climate change indices. The results showed that the number of hot days and nights increased, while the number of cold days and nights decreased. Sajjad and Ghaffar (2018) determined trends of precipitation and temperature by applying CMIP5 GCM simulations to Pakistan. The values of climate extreme indices showed an increasing trend in the number of hot days and of heavy rainfall in the present and future periods.

Climate variables can be thought of as random (Katz & Brown, 1992). Numerous studies have carried out frequency analysis of climate variables such as temperature and precipitation. Most of these studies have used univariate probabilistic functions. Investigating the probability distributions of climatic variables and their extreme values using univariate analysis may lead to miscalculation of risk, given the correlations between variables. Therefore, using multivariate analysis rather than univariate analysis is more appropriate (Dodangeh, Shahedi, Shiau, & Mirakbari, 2017; Grimaldi & Serinaldi, 2006; Mirakbari, Ganji, & Fallah, 2010). Climate parameters do not change independently and can affect each other. Determining the interdependence among these parameters under climate change conditions can help to better assess the risk of extreme events.

To understand the interdependence between climate parameters, it is necessary to determine joint distribution functions. Conventional methods of calculating these functions have limitations

in selecting the type of marginal function, which can cause error in analysis. The copula is a family of multivariate functions that does not suffer from the limitations typical of multivariable distribution functions, as copulas can model the joint distribution of random variables with any marginal function (AghaKouchak, Bardossy, & Habib, 2010; Mesbahzadeh, Miglietta, Mirakbari, Soleimani Sardoo, & Abdolhoseini, 2019; Salvadori & De Michele, 2004; L. Zhang & Singh, 2007). The use of the copula functions in meteorological and hydrological analyses has facilitated multivariate modeling (De Michele & Salvadori, 2003). Recently, copula functions have been used for multivariate analysis of annual peak floods, flood, and drought return periods, and similar climate-related extremes (Bracken, Holman, Rajagopalan, & Moradkhani, 2018; Chen, Zhang, Xiao, Singh, & Zhang, 2016; J. Li, Zhang, Chen, & Singh, 2015; Mesbahzadeh et al., 2019; Mirakbari et al., 2010; Uttam, Goswami, Bhargav, Hazra, & Goyal, 2018; Q. Zhang, Li, Singh, & Xu, 2013). In Iran, many studies have analyzed multivariate modeling of extreme events such as floods and droughts using copulas (Amirataee, Montaseri, & Rezaie, 2018; Azam, Maeng, Kim, & Murtazaev, 2018; Cheraghalizadeh, Ghameshlou, Bazrafshan, & Bazrafshan, 2018; Dodangeh et al., 2017; Mirakbari et al., 2010). However, few studies have been carried out on the joint frequency analysis of climate parameters and their extreme values under climate change conditions. For instance, Uttam et al. (2018) investigated the joint behavior of extreme precipitation by means of climate change indices based on the bivariate copulas in the present and future periods. Joint modeling of temperature and precipitation parameters can help clarify the risk of phenomena such as flood and drought in the future climate change.

Approximately 88% of Iran is arid and semiarid, with generally high temporal variability in temperature and precipitation (Ashraf Vaghefi et al., 2019). There have been few studies on joint modeling of extreme precipitation and temperature under climate change conditions, particularly for arid regions such as central Iran. The country has faced many climate-related disasters, including droughts, floods, and drying lakes and rivers. For instance, the Zayande-Rud river, located in Isfahan province, is at risk of drying. This is the biggest river in central Iran plateau, which supplies the water requirements of different sectors in Isfahan province. Both natural and anthropogenic factors have contributed to the water crisis in the region. Given the impacts of future climate change on extreme events, assessment of joint probabilities of extremes is very important to understand the consequences of future climate change and to provide appropriate strategies in the region. Hence, in this study, precipitation and temperature climate extreme indices were evaluated at Isfahan province, Iran. The main objectives of this study are to (a) evaluate the changes of precipitation and temperature in the historic and future periods; (b) assess changes of climate extremes related to precipitation and maximum temperature; (c) find the proper extreme combinations and the best fit of copula function for joint modeling; (d) determine the conditional probabilities of extreme combinations in the historical period and future period under climate change; and (e) calculate joint return periods of extreme combinations under climate change conditions.

1.1 | Study area

Isfahan province is located in the center of the Iranian plateau (Figure 1). Its eastern parts are located in the western margin of arid and semiarid regions of Iran, while the western regions are on the eastern slopes of the Zagros Mountains. Much of the province experiences semiarid climate with low annual rainfall and high temperatures. The western and southwestern regions of the province have lower temperatures, while the lower eastern and northeastern parts have

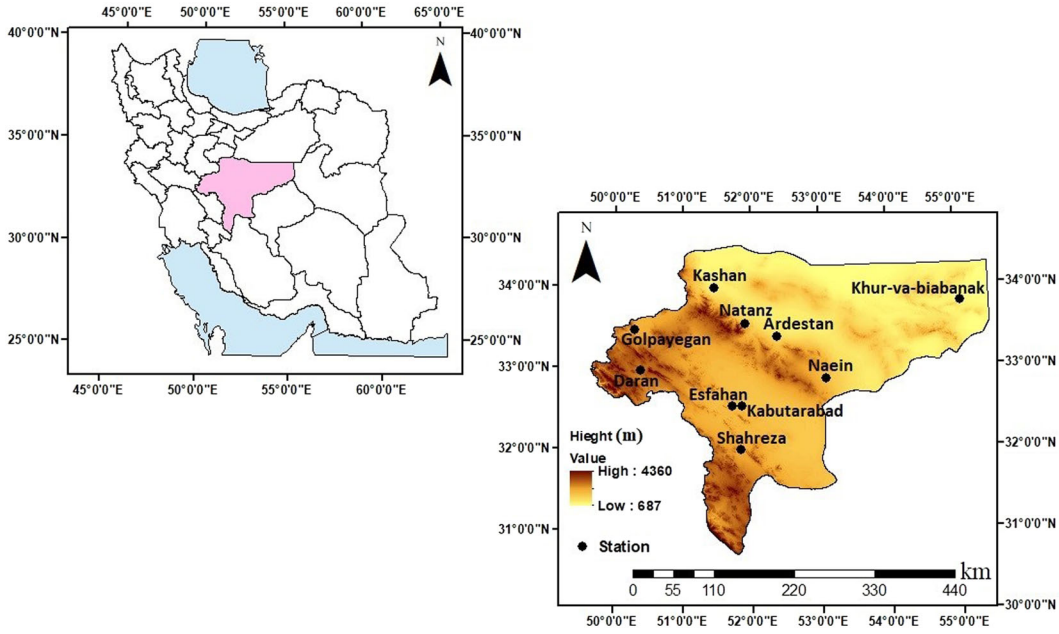

FIGURE 1 Location map of study area and synoptic stations in Isfahan province, central Iran

higher temperatures. The mean annual rainfall in western and eastern parts are 800 and 750 mm, respectively. Precipitation dominantly falls in winter (48.4% of the annual total), autumn (27.6%), and spring (23%), while summers are dry (1%). The average temperature ranges from 16.2°C to 28.2°C in the study region while the average minimum temperature varies from 6.3°C to 1.1°C. The coldest months are January and February, and July and August are the hottest months (Nasri & Modarres, 2009). Figure 2 shows the trend of mean annual precipitation and mean temperature at 10 synoptic stations in Isfahan province. According to the available records, precipitation in the region has a decreasing trend while mean temperature has an increasing trend.

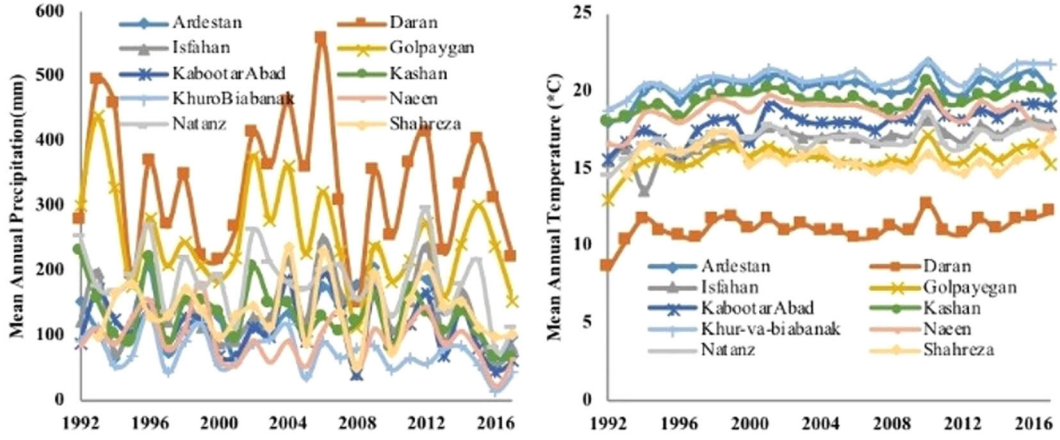

FIGURE 2 Changes in mean annual precipitation (left) and temperature (right) in Isfahan province

2 | MATERIALS AND METHODS

2.1 | Data used

Figure 1 shows the spatial distribution of the stations used in the study area. The main criteria for selecting the stations were length of data coverage and spatial distribution. Maximum daily temperature and daily precipitation data of the selected 10 synoptic stations in Isfahan province (Figure 2) were extracted from the Iranian Meteorological Organization (IMO) data for the period from 1992 to 2017. In addition to the observational data, REMO regional model outputs with a spatial resolution of 0.22° (approximately 25 km), were extracted from the Coordinated Regional Climate Downscaling Experiment (CORDEX; ftp://cccr.tropmet.res.in/iRODS_DATA/CORDEX-Data/REMO2009). REMO is a three-dimensional regional atmospheric model that was developed at the Max Planck Institute for Meteorology in Hamburg, Germany (Pietikäinen et al., 2018). The model is connected to land hydrology and ocean/sea-ice models. The World Climate Research Program (WCRP) initiative CORDEX has generated an ensemble of regional climate change projections by downscaling several GCM outputs using multiple RCMs (Jacob et al., 2012). CORDEX uses dynamic and statistical downscaling methods to provide regional climatic fields (Ujeneza, 2014). CORDEX includes output more than 20 RCMs over the world. REMO has three scenarios, including RCP2.6, RCP4.5, and RCP8.5. We selected RCP4.5 to investigate the impacts of climate change that stabilizes anthropogenic radiative forcing at 4.5 $W\,m^{-2}$ by the year 2100 (Thomson et al., 2011). RCP4.5 corresponds to intermediate greenhouse gas emissions that is considered a medium stabilization scenario.

2.2 | Evaluation of performance of REMO model

The performance of the REMO model was evaluated by coefficient of determination (R^2), percent bias (PBIAS), Nash-Sutcliffe efficiency (NSE), root standard ratio (RSR), and normalized root mean square error (NRMSE; Gupta, Kling, Yilmaz, & Martinez, 2009) for maximum temperature and precipitation parameters during the period of 1992–2005. The performance of REMO was also investigated for extreme indices at stations which the model outputs were in good agreement with observed data using the above criteria.

2.3 | Extreme precipitation and temperature indices

To assess climate change in the study region, 10 climate extreme indices from ETCCDI were computed for the historical and future periods. Table 1 shows the extreme indices used and their definitions. Various thresholds are commonly applied to define extreme temperature and precipitation, generally identified by means of 90th and 95th percentiles of daily temperature and precipitation (Alexander et al., 2006; Erlat & Türkeş, 2013; Graczyk et al., 2017; Moberg & Jones, 2005; Nemec, Gruber, Chimani, & Auer, 2013). In this study, the 90th percentile was considered for maximum temperature. Thresholds defined by ETCCDI were used for precipitation. Heavy and very heavy precipitation were considered as days with more than 10 and 20 mm, respectively. Wet and dry days were also defined as those with precipitation 1 mm or greater and less than 1 mm, respectively.

TABLE 1 Definition of climate indices (extreme precipitation and temperature indices) used in this study

ID	Indicator name	Definition	Unit
SDII	Simple daily intensity index	Average precipitation on wet days	mm/day
PRCPTOT	Annual total wet-day precipitation	Annual total precipitation in wet days (rainfall ≥1 mm)	mm
R10	Number of heavy precipitation days	Annual count of days when precipitation ≥10 mm	Days
R20	Number of heavy precipitation days	Annual count of days when precipitation ≥20 mm	Days
CDD	Consecutive dry days	Maximum number of consecutive days with rainfall <1 mm	Days
CWD	Consecutive wet days	Maximum number of consecutive days with rainfall ≥1 mm	Days
R95p	Very wet days	Annual total precipitation when rainfall >95th percentile	mm
Su30	Number of summer days	Annual count of days when daily maximum temperature >30°C	Days
WSDI	Warm spell duration indicator	Annual count of days with at least 6 consecutive days when TX >90th percentile	Days
Id	Number of icing days	Annual count of days when daily maximum temperature <0°C	Days

2.4 | Copula theory

Sklar (1959) introduced copula theory. Copulas are functions that can be used to create a joint distribution of two or more variables regardless of the type of marginal function. Thus, assuming that two extreme precipitation or maximum temperature indicators are considered as random variables X and Y respectively, a joint distribution with joint cumulative probability p is defined by C (Equation (1)) (Nelsen, 2006).

$$P(X \le x,\ \ Y \le y) = C[F(X),\ \ F(Y)] = p. \tag{1}$$

Here, C is a copula function and $F(X)$ and $F(Y)$ are the marginal distributions of the random variables X and Y. Copula functions model the dependence structure of random variables given separate marginal distributions. Copulas come in several families, of which the Archimedean and Elliptical families are the most commonly used (Madadgar & Moradkhani, 2013). The Archimedean family has symmetric and asymmetric forms, which respectively, have one parameter and more than two parameters. The Elliptical family does not follow one specific form. In this study, the symmetric Archimedes copulas (Frank, Gumbel, and Clayton) and an Elliptical copula (Gaussian) were used for the bivariate modeling of the extreme maximum temperature and precipitation.

Akaike information criteria (AIC; Equation (2)) and Bayesian information criteria (BIC; Equation (3)) were used to select the best-fitting copula (Akaike, 1974). The ordinary least squares (OLS) method was used to compare the empirical copula with theoretical copulas (R. Li & Geng, 2013). The OLS method determines the best copula based on the squared difference between the empirical and the theoretical probability values (Equation (4)). The empirical copula is estimated based on the joint behavior of random variables (X, Y) with respect to the joint

cumulative distribution of variables ($F(X)$, $F(Y)$) on the interval $l \in [0, 1]$, without considering any theoretical marginal distribution (Equation (5)) (Genest, Favre, Liveau, & Jacques, 2007).

$$\mathrm{AIC} = 2k - 2\ln(L), \tag{2}$$

$$\mathrm{BIC} = 2n\mathrm{Log}L + k\mathrm{Log}(n), \tag{3}$$

$$\mathrm{S_{OLS}} = \sqrt{\frac{1}{n}\sum_{i=1}^{n}(P_{ei} - P_i)^2}, \tag{4}$$

$$C_n(F(X),\ F(Y)) = \frac{1}{n}\sum_{i=1}^{n} I\left(\frac{r_{F(x)i}}{n+1} \le F(X),\ \ \frac{r_{F(y)i}}{n+1} \le F(Y)\right), \tag{5}$$

where P_{ei} are the empirical copula values, $_{Pi}$ are the theoretical copula values, k is a model parameter, n is the number of observations, and L is the maximum likelihood function value, $r_{F(x)i}$ and $r_{F(y)i}$ are the ranks of x_i and y_i, and $I(A)$ is the logical indicator function of set A (0 if A is false, 1 if A is true). Both nonparametric and parametric methods were used to estimate the parameters of the copula functions. The nonparametric estimation used the relationship between the generator function of each copula and the Kendall correlation coefficient (Equation (6); Genest, Favre, Liveau, & Jacques, 2007). In the parametric method, the θ parameter was estimated using the maximum log-likelihood function (Equation (7); Favre, El Adlouni, Thi Emong, & Bobee, 2004), in which c_θ is the Copula density function, F is the marginal distribution function and $x_{1k},\ \ x_{2k}, ..., x_{pk} (k = 1, ..., n)$ are the dependent random variables.

$$\tau(X,\ Y) = 1 + 4\int_0^1 \frac{\varphi(\upsilon)}{\varphi'(\upsilon)} d\upsilon, \tag{6}$$

$$L(\theta) = \sum_{k=1}^{n} \log\left[c_\theta\{F_1(x_{1k}), ..., F_p(x_{pk})\}\right]. \tag{7}$$

2.5 | Copula-based conditional probability

Conditional probabilities of any combination of random variables is easily computed given their joint distribution. Thus, conditional probability is obtained from the copula functions as the threshold level for any combination of extreme precipitation and temperature. In other words, if we need to know the probability of a variable x equaling or exceeding some value given that the variable y is greater than or equal than a certain threshold level, this can be obtained by calculating the conditional probability on the basis of copula theory (Equation (8); Shiau, 2006). Conversely, knowing the probability for the variable y, given that the variable x exceeds a certain threshold, is indicated by Equation (9) (Shiau, 2006).

$$P(X \le x \,|\, Y \ge y') = \frac{F_X(x) - F_{X,\ Y}(y',\ \ x)}{1 - F_Y(y')} = \frac{F_Y(y') - C(F_Y(y'),\ \ F_X(x))}{1 - F_Y(y')}, \tag{8}$$

$$P(Y \le y \,|\, X \ge x') = \frac{F_Y(y) - F_{X,\ Y}(x',\ \ y)}{1 - F_Y(y')} = \frac{F_X(x') - C(F_X(x'),\ \ F_Y(y))}{1 - F_X(x')}. \tag{9}$$

2.6 | Copula-based joint return period

A copula-based joint return period can be used to overcome under- or over-estimates of risk related to extreme events such as floods and droughts. The return period is described as the average interval between successive events (Liu et al., 2015; Uttam et al., 2018). Assuming that x and y are the extreme value thresholds of climatic parameters with the copula function ($C(F_X(X), F_Y(Y))$, the joint return period of the two variables, when both the X and Y variables exceed a certain value ($T(X \geq x, Y \geq y)$) is defined as

$$T_{XY} = T(X \geq x, \ \ Y \geq y) = \frac{1}{P(X \geq x, \ \ Y \geq y)} = \frac{1}{1 - F_X(x) - F_Y(y) + C(F_X(x), \ \ F_Y(y))}. \tag{10}$$

3 | RESULTS

3.1 | Performance evaluation of REMO model

To evaluate the REMO model at the study region, the model outputs were compared with observational data for the period of 1992–2005 using evaluation criteria for all 10 synoptic stations. According to the finding of this section, the REMO model had acceptable performance for the maximum temperature and precipitation parameters only for three stations, Naeen, Daran, and Shahreza (Table 2). The REMO data were in a good agreement with observed precipitation and maximum temperature at these stations based on NSE, PBIAS, RSR, R^2, and NRMSE criteria. According to the De Martonne's climatic classification, the selected stations

TABLE 2 Evaluation criteria of REMO for precipitation and maximum temperature in synoptic stations, Isfahan province

Parameter	Station	NSE	PBIAS	RSR	R^2	NRMSE
Precipitation	Isfahan	0.012	10.2	0.99	0.29	0.12
	Daran	0.75	0.13	0.49	0.95	0.049
	Ardestan	0.25	12.3	0.87	0.21	1.02
	Khur-va-Biabanak	−0.79	−0.9	1.34	0.49	0.138
	Golpaygan	0.21	0.37	0.821	0.31	0.083
	Kabutar Abad	0.178	−0.051	0.91	0.23	0.851
	Naeen	0.71	−0.012	0.55	0.75	0.671
	Kashan	0.28	−0.48	0.841	0.42	0.102
	Shahreza	0.638	−0.034	0.54	0.72	0.074
Maximum temperature	Isfahan	−1.031	−0.691	1.42	0.153	0.172
	Daran	0.991	0.006	0.092	0.962	0.009
	Ardestan	0.086	−2.01	0.92	0.25	0.452
	Khur-va-Biabanak	−0.59	−0.25	1.02	0.51	0.124
	Golpaygan	0.65	0.077	0.185	0.85	0.0181
	Kabutar Abad	0.58	0.131	0.32	0.71	0.21
	Naeen	0.971	0.0381	0.159	0.73	0.016
	Kashan	0.38	−0.78	0.714	0.49	0.12
	Shahreza	0.982	0.029	0.132	0.793	0.0142

Note: The three stations with best correspondence between observations and REMO output are highlighted in bold.
Abbreviations: NRMSE, normalized root mean square error; NSE, Nash-Sutcliffe efficiency; PBIAS, percent bias; RSR, root standard ratio; R^2, coefficient of determination.

have different climatic classes (De Martonne, 1925): the Daran station is in the semihumid class, Shahreza is Mediterranean, and Naeen is in the dry class (Figure 3).

The comparison of performance evaluation criteria for extreme indices at these three stations (i.e., Daran, Naeen, and Shahreza) showed that the REMO outputs were in agreement with the historical extreme indices (Table 3). Therefore, it can be concluded the REMO model has suitable performance for assessing changes in extreme climate in the future for at least the selected stations in the study region.

Table 4 shows the trends for precipitation and maximum temperatures in the historical period (1992–2017) and future period (2020–2100) based on the Mann–Kendall nonparametric trend test (Kendall, 1975; H. B. Mann, 1945). There was no significant trend for precipitation in either the historical and or future periods. However, the maximum temperature in the stations of Daran and Shahreza in the historical period and all three stations in the future period have a significant increasing trend. Precipitation in both Daran and Shahreza stations is simulated by REMO to decrease by 22.7% and 33.3%, respectively, in the future period, while at Naein station precipitation increases by 2.01%. Maximum temperature in all three stations, Daran, Naeen, and Shahreza, will increase, by 8.13°C, 5.66°C, and 6.58°C, respectively, compared to the historical period.

3.2 | Climate change indicators

3.2.1 | Extreme precipitation indicators

Annual values of the indicators PRCPTOT, R10, R20, consecutive wet days (CWD), consecutive dry days (CDD), SDII, R95p were obtained using the RClimDex software for each station in the

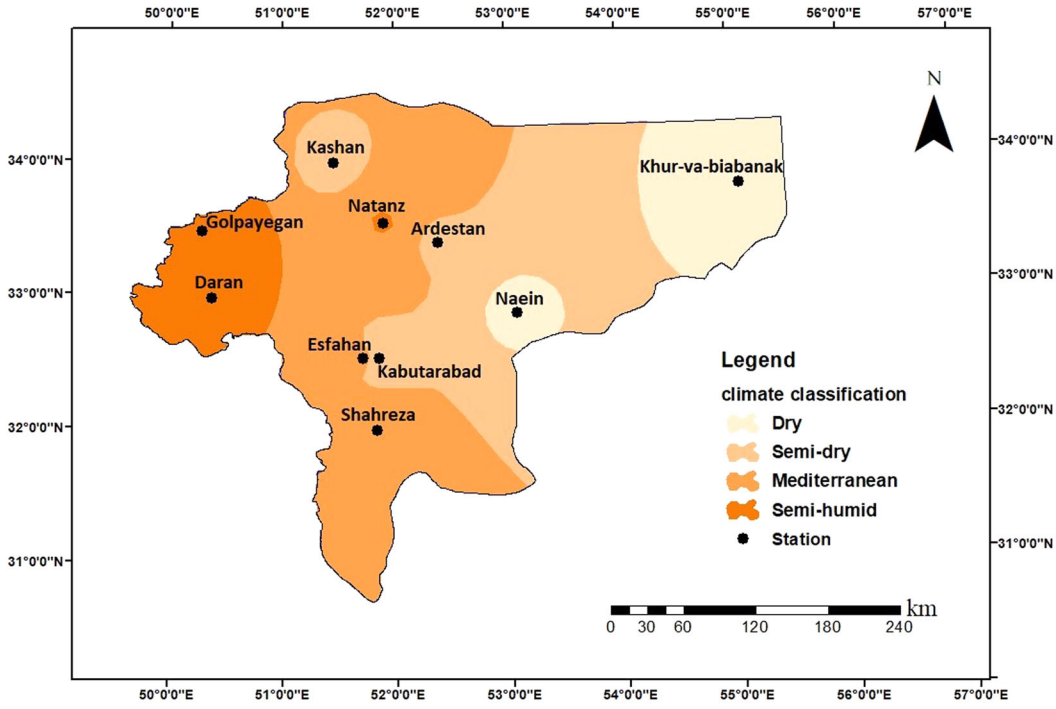

FIGURE 3 De Martonne classification of Isfahan province study area

TABLE 3 Evaluation criteria of REMO for extreme indices at Daran, Naeen, and Shahreza stations in the historical period

Stations	Indices	NSE	PBIAS	RSR	R^2	NRMSE
Daran	SDII	0.52	0.3	0.48	0.85	0.19
	PRCPTOT	0.59	0.37	0.44	0.5	0.049
	R10	0.55	0.23	0.2	0.82	0.14
	R20	0.61	0.13	0.43	0.78	0.01
	CDD	0.64	0.20	0.48	0.71	0.27
	CWD	0.51	0.14	0.63	0.8	0.2
	R95p	0.42	1.54	0.6	0.57	0.8
	Su30	0.79	2.54	0.19	0.75	0.54
	WSDI	0.84	0.02	0.1	0.89	0.21
	Id	0.78	0.12	0.17	0.81	0.47
Naeen	SDII	0.56	−1.25	0.59	0.65	1.71
	PRCPTOT	0.49	2.51	0.64	0.56	2.14
	R10	0.53	0.43	0.49	0.62	1.02
	R20	0.47	2.04	0.61	0.68	0.97
	CDD	0.501	3.12	0.49	0.49	2.45
	CWD	0.5	1.97	0.58	0.61	1.33
	R95p	0.62	0.54	0.45	0.67	0.12
	Su30	0.68	3.04	0.31	0.65	1.84
	WSDI	0.81	0.34	0.15	0.78	0.08
	Id	0.78	0.22	0.28	0.69	0.19
Shahreza	SDII	0.63	−0.04	0.54	0.61	1.07
	PRCPTOT	0.59	−3.51	0.54	0.64	1.47
	R10	0.49	1.71	0.59	0.501	0.98
	R20	0.50	1.05	0.47	0.61	1.56
	CDD	0.39	4.13	0.67	0.44	2.67
	CWD	0.45	−4.78	0.57	0.55	3.05
	R95p	0.42	1.90	0.55	0.47	1.64
	Su30	0.53	1.84	0.38	0.52	2.35
	WSDI	0.79	0.24	0.22	0.88	0.14
	Id	0.87	0.18	0.17	0.89	0.015

Abbreviations: NRMSE, normalized root mean square error; NSE, Nash-Sutcliffe efficiency; PBIAS, percent bias; RSR, root standard ratio; R^2, coefficient of determination.

TABLE 4 Annual changes trend of precipitation and maximum temperature for historical (1992–2017; Observed) and future (2020–2100; RCP4.5) periods

		Z value		
Parameter	Station	Observed	RCP4.5	Change %
Precipitation	Daran	−0.44	−0.852	−22.7
	Naeen	−1.24	0.445	+2.01
	Shahreza	−0.44	−0.627	−33.3
Maximum temperature	Daran	**1.85**	**5.23**	+42.3
	Naeen	0.176	**5.15**	+23.3
	Shahreza	**−1.65**	**5.59**	+29.53

Note: Bold values show significant trend at 10% level.

base and future periods. RClimDex was developed by the Canadian Meteorological Institute (X. Zhang & Yang, 2004). This software is used to obtain climatic extreme indices as discussed in X. Zhang, Hegerl, Zwiers and Kenyon (2005b) and Haylock et al. (2006). To determine the changes of extreme precipitation in the future compared to the current period, temporal differences in the climate extreme indices were obtained. The results revealed that Daran station with semihumid climate and Naeen with arid climate had the highest and lowest changes of extreme precipitation, respectively (Table 5). The PRCPTOT and R95p indices had the highest changes compared to other extreme precipitation indices for the future period. Based on the values obtained from SDII, PRCPTOT, R10, R20, R95p, CDW indices at Daran and Shahreza stations, the extreme precipitation index values will decrease in the future compared to the current period. However, at Naeen station, extreme precipitation indices of PRCPTOT, CDD, and CWD will decrease in a more limited way, and SDII, R10, R20, and R95p indices will even increase in the future period. Trends in extreme precipitation occurrences were also quantified using the Mann–Kendall test for the historical and future periods. Table 5 shows the Z values of the Mann–Kendall test for extreme precipitation indices. The results of the Mann–Kendall test indicated a decreasing trend for most extreme precipitation indices over the historical period, meaning the study region has been experiencing a decrease in intense precipitation. In the future, the SDII and CDD indices at Daran stations are simulated to undergo a significant increasing trend. In contrast, the other extreme indices do not show significant trends.

4 | EXTREME MAXIMUM TEMPERATURE INDICES

The annual series of extreme maximum temperature indices SU30, WSDI, Id were calculated for the historic and future periods (Table 6). The results showed that similar to the extreme precipitation indices, the future extreme maximum temperature values at Naeen and Daran stations were simulated to show the smallest and largest changes, respectively. The WSDI and SU30 indices will have positive changes in the future period, while the Id index has a negative change. The Mann–Kendall trend test indicated that the SU30 and WSDI indices have a significant upward trend in all stations in the future period, while Id in both periods, present and future, has a decreasing trend that will only be significant for the future period at Daran station (Table 6). Based on the extreme maximum temperature indices, the increasing trend of temperature in the study region for both study periods is evident.

4.1 | Joint analysis by copula theory

4.1.1 | Determining the best-fitted copula

One of the most important tasks in fitting the copula functions for joint modeling is the creation of trend-free stationary time series (Benth & Saltyte-Benth, 2005; Cong & Brady, 2012; Pandey et al., 2018). For this purpose, an autocorrelation test was performed using the autocorrelation function (ACF) for the extreme precipitation and maximum temperature series. Autocorrelation is the correlation between time series at different points in time as a function of time difference. Therefore, if there is autocorrelation, the variance of the residuals and the estimated coefficients may increase compared with no autocorrelation, which will reduce the model performance (Cong & Brady, 2012). Based on the generated ACF plots, there was no significant autocorrelation in the extreme precipitation and maximum temperature time series. For the

TABLE 5 *Z* values of Mann–Kendall trend test for extreme precipitation indices in historical and future periods and changes of extreme precipitation

	Daran			Naeen			Shahreza		
Indices	**Observed**	**RCP4.5**	**Changes**	**Observed**	**RCP4.5**	**Changes**	**Observed**	**RCP4.5**	**Changes**
SDII	0.751	**1.84**	−2.39	−1.09	1.38	0.43	−0.34	0.17	−1.52
PRCPTOT	−0.39	−0.82	−69.68	−1.42	0.61	−0.029	−0.81	−0.55	−41.52
R10	−0.80	−0.54	−5.22	−1.25	1.25	0.005	0.05	0.79	−2.25
R20	0.15	0.324	−2.29	0.85	1.53	0.41	−1.08	−0.39	−0.8
CDD	0.71	**2.09**	−34.4	−0.71	−0.27	−2.07	0.57	1.03	−31.1
CWD	−0.83	−1.16	1.05	0.14	−0.039	−0.027	−1.23	−1.27	0.31
R95p	0.93	1.19	−39.17	−0.53	1.29	10.58	−1.03	−0.61	−13.21

Note: Bold values show significant trend at 10% level.

TABLE 6 *Z* values of Mann–Kendall trend test for maximum extreme temperature indices in historical and future periods and changes of extreme maximum temperature

	Daran			Naeen			Shahreza		
Indices	**Observed**	**RCP4.5**	**Changes**	**Observed**	**RCP4.5**	**Changes**	**Observed**	**RCP4.5**	**Changes**
Su30	1.19	**5.0**	28.65	**2.69**	**4.33**	1.87	0.86	**4.6**	0.67
WSDI	**2.25**	**5.12**	65.42	**3.06**	**4.98**	24.5	**1.7**	**4.9**	20.51
Id	**−1.67**	**−2.61**	−2.28	−0.19	−0.61	1.46	−1.2	−1.44	2.74

Note: Bold values show significant trend at 10% level.

bivariate analysis, the correlation of different combinations of extreme precipitation and extreme maximum temperature was determined by Kendall rank correlation coefficient for both study periods. Based on Kendall coefficient values, pairs of variables obtained from the extreme precipitation had the highest correlation; these were then selected for bivariate analysis. Table 7 shows the Kendall's tau correlation of the extreme combinations selected for the bivariate analysis by copula theory in the historic and future periods.

For the bivariate analysis, the marginal distribution of the individual extreme precipitation indicators was selected using the Kolmogorov–Smirnov and Anderson–Darling tests (Modaresi Rad, Ghahraman, Khalili, Ghahremani, & Ahmadi Ardakani, 2017). To confirm the selective marginal functions, the AIC was applied (Modaresi Rad et al., 2017; Onoz & Bayazit, 2003). Table 8 lists the best-fitted marginal functions of extreme precipitation at each station.

TABLE 7 Kendall's tau values of pair variables with highest correlation in base period and future period

	Daran		Naeen		Shahreza	
Combination	**Observed**	**RCP45**	**Observed**	**RCP45**	**Observed**	**RCP45**
(R10, PRCPTOT)	0.77	0.70	0.75	0.71	0.75	0.64
(R10, SDII)	0.524	0.58	0.76	0.68	0.67	0.70
(R95p, R10)	0.44	0.40	0.54	0.50	0.53	0.51
(SDII, R95p)	0.60	0.61	0.57	0.51	0.64	0.56
(SDII, PRCPTOT)	0.53	0.53	0.71	0.69	0.59	0.58
(CWD,R10)	–	–	0.40	0.41	–	–
(CWD,PRCPTOT)	–	–	–	–	0.38	0.41

TABLE 8 List of the best fit marginal functions of extreme precipitation in historical and future periods

	Daran		Naeen		Shahreza	
Extreme precipitation	**Observed**	**RCP4.5**	**Observed**	**RCP4.5**	**Observed**	**RCP4.5**
R10	Weibull(2p)	Gumbel	Gumbel	GEV	Normal	GEV
R95p	Exponential	GEV	GEV	GEV	GEV	Gumbel
PRCPTOP	Weibull(2p)	Gumbel	Normal	Generalized Gamma	Normal	Gumbel
SDII	Gamma(2p)	LP3	Gumbel	Generalized Gamma	Gamma	LN(2p)
CWD	–	–	GEV	GEV	LN(3p)	LN(2p)

The parameter of the copulas was estimated by both parametric and nonparametric methods for extreme combinations and then the best fit copula was selected on the basis of the AIC, BIC, and OLS criteria. According to these criteria, the parametric method resulted in better estimation than the nonparametric method, consistent with previous work (Dodangeh et al., 2017; Mesbahzadeh et al., 2019; Mirakbari et al., 2010). Among the five fitted copula functions at the Daran station, the Gaussian copula was used to jointly model the combinations of (R10, SDII), (R10, PRCPTOT), (SDII, PRCPTOT), and the Frank, and Gumbel Copulas were used for the combinations of (R95p, SDII) and (R95, R10), respectively, in the historical period. In the future period, the Gumbel copula was chosen for combinations of (R95p, SDII), (R10, PRCPTOT), (R10, R95p), and the Frank and Gaussian copulas were chosen for (R10, SDII) and (SDII, PRCPTOT), respectively. At Naeen station, the Gaussian copula was chosen for the combinations of (R10, SDII), (R10, PRCPTOT), (SDII, PRCPTOT), and (R95p, SDII) and the Frank and Gumbel copulas were chosen for (CWD, R10) and (R10, R95p), respectively, in the historical period. At Shahreza station, the Gaussian copula was selected for combinations of (R10, PRCPTOT), (R10, R95p), (SDII, PRCPTOT), (R95p, SDII), (CWD, PRCPTOT) in the historical and future periods. The Clayton and Gumbel functions for combination of (R10, SDII) were also selected in base period and future period (Table 9).

Differences in the type of copulas fitted in the historical and future periods suggested that the joint behavior of the extreme precipitation values in the future period projection is different from the historical period.

4.2 | Conditional probability of extreme precipitation

Conditional probability was obtained by assigning three threshold levels with probability of 0.1, 0.3, and 0.9 for the extreme precipitation combinations of SDII, PRCPTOT, R10, R95p, and CWD using Equations (8) and (9). Figure 4 shows the conditional probability of these combinations for certain thresholds at Daran and Shahreza stations. For example, based on the derived conditional distribution at Daran, the probability for the precipitation intensity (SDII) less than 7.98 mm/day ($P(SDII) < 0.5$) given the total annual precipitation (PRCPTOT) exceeding 290.83 mm ($P(PRCPTOT) \geq 0.4$) is equal to 0.28 in historical period. In the future period, the probability for SDII < 5.74 mm/day (corresponding to probability of less than 0.5 ($P(SDII) < 0.5$)) given the PRCPTOT ≥ 291 mm (corresponding to probability of annual precipitation greater than or equal to 0.4, $P(PRCPTOT) \geq 0.4$) is equal to 0.3. For the historical and future periods, respectively, the probabilities for heavy precipitation on less than 11 and 5.7 days (corresponding to probability of less than 0.5 ($P(R10) < 0.5$)) given the total annual precipitation exceeding 291 and 219 mm (corresponding to probability of less than 0.4 ($P(PRCPTOT) < 0.5$))) are equal to 0.33 and 0.37, respectively. The values of conditional probabilities revealed that extreme precipitation indices have a different behavior in the base and future periods. As a consequence, some extreme combinations had greater conditional probability in historical period than in future period, whereas it was the opposite for some other combinations. Generally, at higher threshold values, the probability of extreme precipitation increases (Figure 4).

4.3 | Copula-based bivariate return period of extreme precipitation

The bivariate return period of extreme precipitation combinations for the historical and future periods were calculated based on Equation (10) using the selected copulas. Based on Equation (10),

TABLE 9 Best selected copula based on evaluation criteria for extreme precipitation combinations in historical and future periods

	Daran				Naeen				Shahreza			
Extreme precipitation	**Copula**	**AIC**	**BIC**	**S_{OLS}**	**Copula**	**AIC**	**BIC**	**S_{OLS}**	**Copula**	**AIC**	**BIC**	**S_{OLS}**
Historical												
(R10, PRCPTOT)	Gaussian	−15.3	−13.2	0.85	Gaussian	−32.8	−31.2	0.87	Gaussian	−18.1	−17.3	0.28
(R10, SDII)	Gaussian	−17.6	−15.8	0.57	Gaussian	−33.4	−31.5	0.24	Clayton	−25.4	24.5	0.47
(R95p, R10)	Gumbel	−12.8	−11.5	0.87	Gumbel	−11.3	−10.2	0.35	Gaussian	−9.65	−8.4	0.51
(SDII,R95p)	Frank	−19.5	−17.2	0.24	Gaussian	−30.3	−28.1	0.27	Gaussian	−17.3	−15.6	0.54
(SDII, PRCPTOT)	Gaussian	−23.7	−21.7	0.35	Gaussian	−32.8	−31.4	0.79	Gaussian	−19.9	−17.5	0.64
(CWD,R10)	–	–	–	–	Frank	−4.1	−3.4	0.57	–	–	–	–
(CWD, PRCPTOT)	–	–	–	–					Gaussian	−4.51	−3.54	0.87
RCP4.5												
(R10, PRCPTOT)	Gumbel	−99.3	−90.2	0.88	Gaussian	−105.9	−100.1	0.77	Gaussian	−83.5	−82.4	0.24
(R10, SDII)	Frank	−66.9	−58.7	0.67	Frank	−85.9	−84.3	0.37	Gumbel	−92.3	−90.7	0.57
(R95p, R10)	Gumbel	−22.5	−21.4	0.87	Gaussian	−91.6	−90.5	0.45	Gaussian	−34.1	−33.7	0.56
(SDII,R95p)	Gumbel	−77.1	−68.1	0.34	Frank	−87.2	−86.4	0.37	Gaussian	−45.4	−44.7	0.44
(SDII, PRCPTOT)	Gaussian	−61.7	−57.2	0.38	Clayton	−68.6	−66.1	0.87	Gaussian	−77.4	−76.8	0.74
(CWD,R10)	–	–	–		Gumbel	−53.9	−51.4	0.68	–	–	–	–
(CWD, PRCPTOT)	–	–	–						Gaussian	−24.9	−22.9	0.25

Abbreviations: AIC, Akaike information criteria; BIC, Bayesian information criteria.

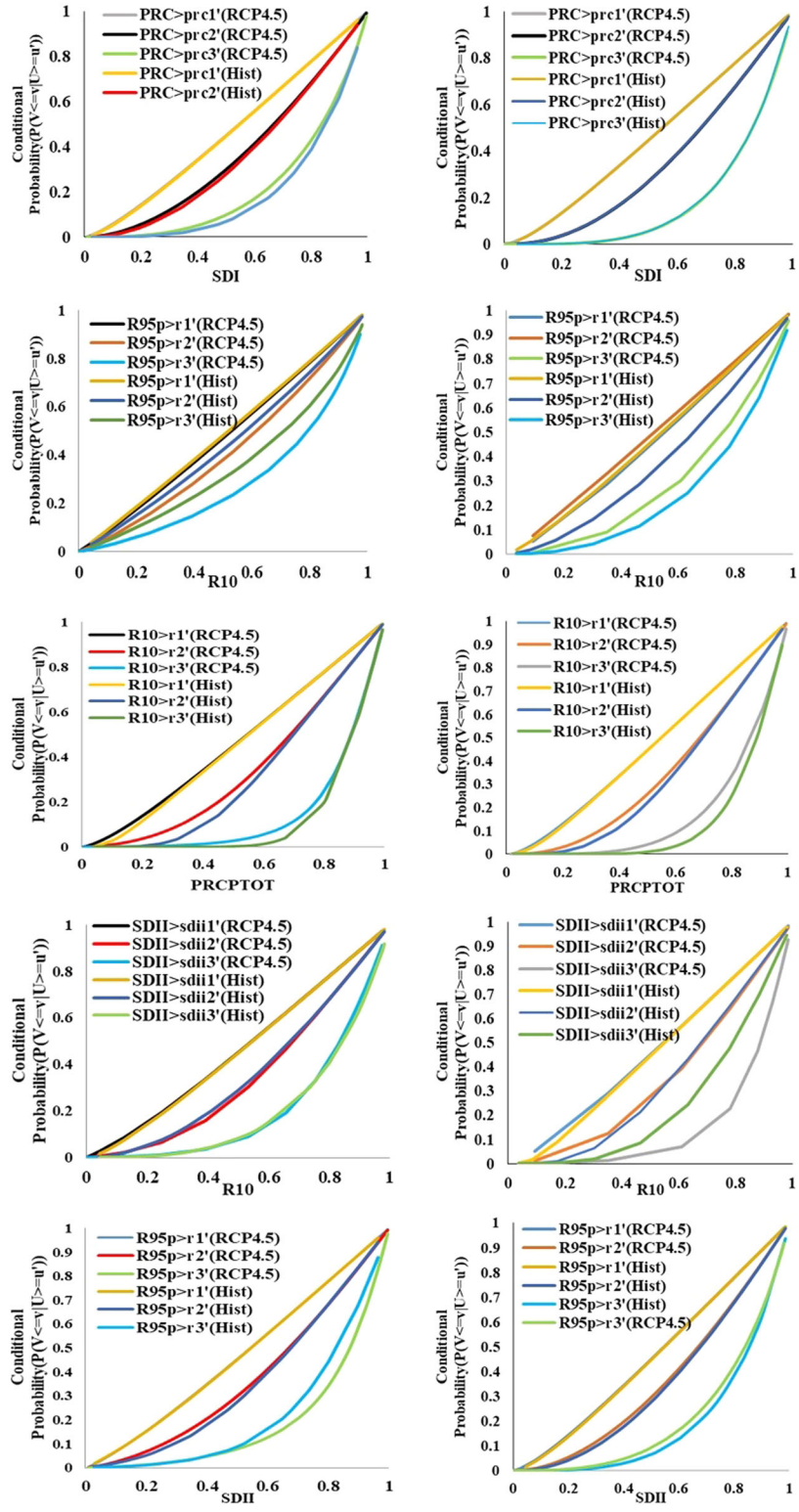

FIGURE 4 The conditional probability of extreme precipitation in historical and future periods given PRCPTOT (a), R95p(b), R10(c), SDII(d,e) exceeding a certain value, u' at Daran (left) and Shahreza (right) stations

the return period of the various extreme combinations that simultaneously exceed a certain value is provided. The results showed that the mean interval of extreme precipitation occurrence in the historical and future periods varied for different combinations. In other words, the return period of different combinations of extreme events in the future will change compared to the historical period. For example, at Daran station, the average return periods of combination of (SDII, PRCPTOT) in present and future periods were 21 and 12 years, respectively. This means that different amounts of precipitation intensity (SDII) and total annual precipitation (PRCPTOT) may simultaneously occur on average every 21 years in the historical period and every 12 years in the future. Based on other joint return period values of extreme combinations, the average return periods of (R10, SDII), (R95p, SDII), (R10, PRCPTOT), and (R10, R95p) in the historical period were 13, 15, 22, and 21 years, respectively and 5, 9, 10, and 7 years for the future period. The future return periods will be approximately 50% less than the historical period. Also, the results of return period at Shahreza station showed the average joint return period for combinations of (R10, SDII), (R95p, SDII), (R10, PRCPTOT), (SDII, PRCPTOT), (R95p, R10), and (CWD, PRCPTOT) will reduce by 50%, 50%, 27%, 16%, 47%, and 6%, respectively, as compared to the historical period. The findings of joint return period of various extreme combinations revealed that the risk of drought (water supply shortage) will likely be higher in future than in the historical period. In contrast, the study region may experience fewer floods in the future. At Naeen station, the values of joint return period were different than the other two stations. There, the future average return period of combinations of (R10, PRCPTOT) (R10, R95p) (CWD, R10) will reduce by 39%, 11%, and 44% compared to the historical period, while the average return period of (R10, SDII) (R95p, SDII)) (SDII, PRCPTOT) will increase by 33–70% in the future, respectively. Figures 5 and 6 show contour lines of the joint return period at Daran and Shahreza stations in the historical period (1992–2017) and future (2020–2100).

5 | DISCUSSION AND CONCLUSIONS

The purpose of this study was to investigate trends of climate parameters based on climate extreme indices in the present and future periods using the REMO regional model. R10, R95p, SDII, PRCPTOT, CWD, CDD, and R20 extreme indices were used to investigate the changes of precipitation extreme values over the historical period (1992–2017) and the future period (2020–2100) under RCP4.5 scenario. Also, Id, SU30, and WSDI extreme indices were considered to investigate the changes in extreme maximum temperature. Extreme precipitation values in the historical and future periods had increasing and decreasing variations, while only CDD and SDII indices had a significant increasing trend under the RCP4.5 scenario at Daran station. Changes of extreme precipitation at Daran and Shahreza stations showed that the precipitation intensity (SDII), total annual precipitation (PRCPTOT), heavy precipitation (R10), very heavy precipitation (R20), very humid days (R95P), and maximum CDDs will decrease in the future as compared to the current period. However, the maximum CWD at all three stations will increase relative to the current period. The reduction of the extreme precipitation indices of SDII, PRCPTOT, R10, R20, and R95p indicated that the study region will experience less intense precipitation in the future. These conditions may increase the occurrence probability of drought in the study region. The assessment of changes in temperature showed a significant increasing trend over the historical and future periods that confirm the impact of global warming on the regional scale. The extreme maximum temperature indices SU30, WSDI, and Id confirm the increase in temperature over the historical and future periods. Therefore, based on the results of extreme precipitation and

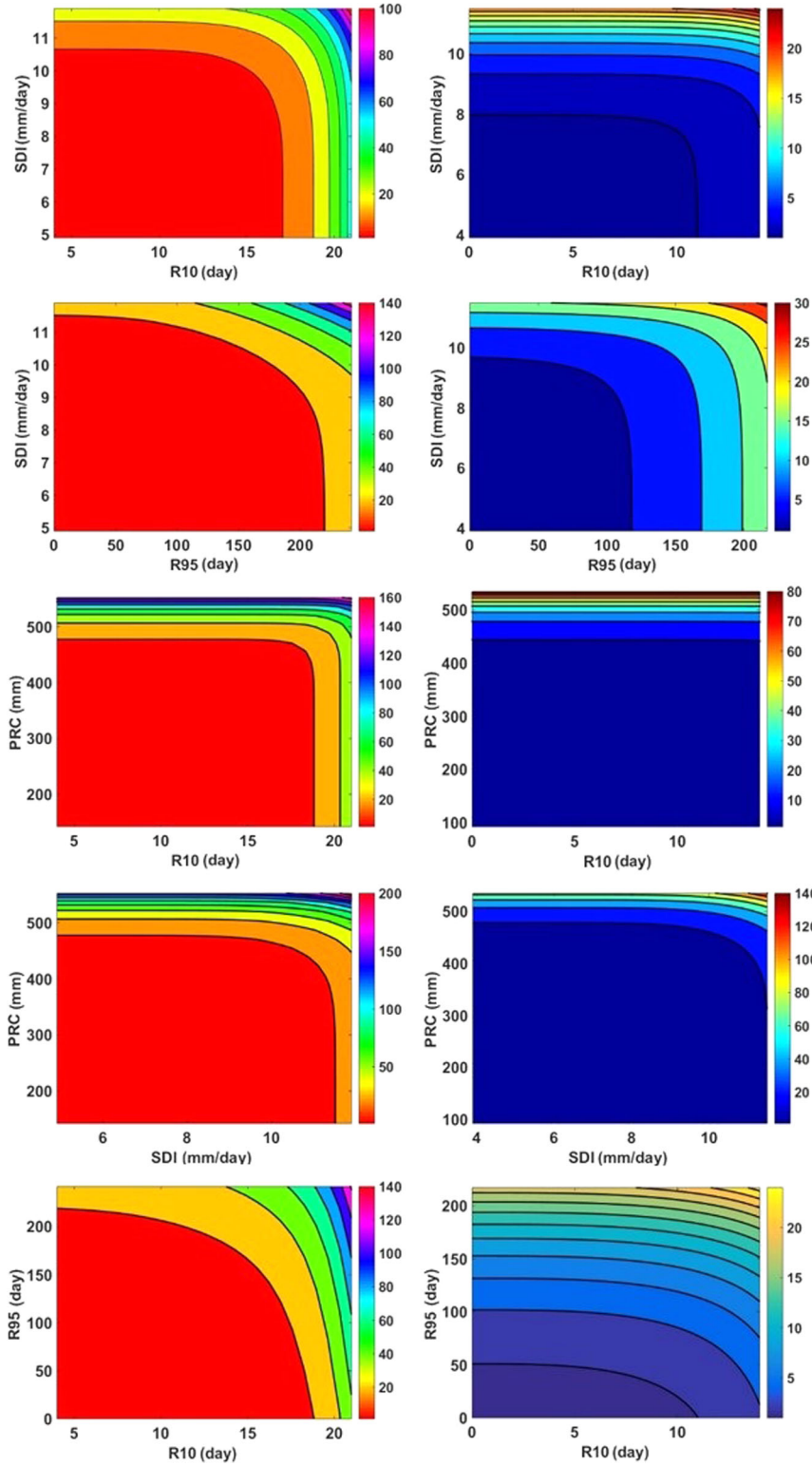

FIGURE 5 Bivariate return period ($RT(X \geq x, Y \geq y)$) of extreme precipitation in historical (left) and future (right) period at Daran station

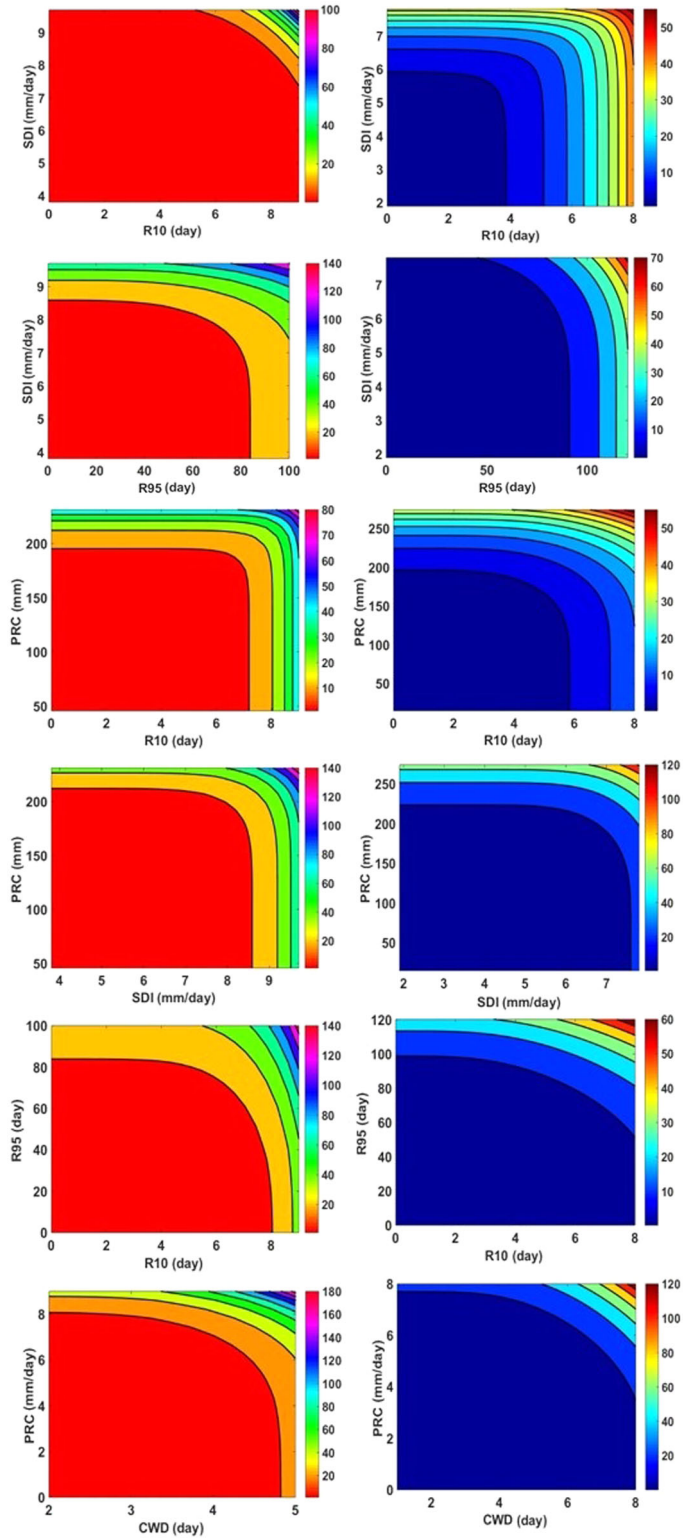

FIGURE 6 Bivariate return period ($RT(X \geq x, Y \geq y)$) of extreme precipitation in historical (left) and future (right) period at Shahreza station

maximum temperature, it can be concluded that the precipitation changes and the increasing temperature will affect water resources, and may decrease the future reliability of water reservoirs in the study region. In general, the occurrence of drought will be more likely. Climate extremes are particularly important because the increasing or decreasing trend of extreme precipitation and temperature can have a potential impact on natural disasters such as floods and droughts, as well as on water resources and civil infrastructure.

Joint modeling of extreme precipitation based on copula theory in the historical and future periods was performed by fitting candidate copulas such as Gaussian, Frank, Gumbel, and Clayton. The combinations of extreme precipitation were selected for joint analysis because of their higher correlation between different indicators relative to extreme temperature. The selected copulas indicate that different extreme combinations have different tail dependences. For instance, at Daran station (historical period), the selected Frank and Gaussian copulas for combinations of (R10, PRCPTOT), (R10, SDII), (SDII, PRCPTOT), and (SDII, R95) show no dependency in the upper or lower tails of the joint distributions. However, for the combination of (R10, R95), the Gumbel copula is selected, which shows dependency at the upper tail. Moreover, the Clayton copula, with lower-tail dependence, was selected for the combination of (R10, SDII) at Shahreza. Conditional probabilities were obtained by the best-fitted copulas for different extreme combinations. From the conditional probability values, water resource managers can be informed of the occurrence probability of different combinations of extreme precipitation that exceed certain thresholds. This information will help planning for water resource systems under future increasing temperature. Assessment of joint return period of extreme events is important to water resources and land management. Indeed, joint return period is a useful tool to develop effective strategies for water resources allocation. Based on the average joint return period of (R10, SDII), (R95p, R10), (R10, PRCPTOT), (SDII, PRCPTOT), and (CWD, PRCPTOT), the average interval time between combined extreme precipitation events will decrease in the future compared to historical period at Daran and Shahreza. The decreasing joint return period can imply that the risk of extreme events will increase under future climate change. Therefore, due to the dependency of agriculture, industry, and drinking water of Isfahan province on the Zayande-Rud river and also the decreasing return period of extreme precipitation combinations, the importance of water resources management will increase in the study region, and instability of water resources may potentially intensify in the study region.

In general, the results of this study are important to assess the prediction of climate extremes as mean climate conditions change in the future. Also, these findings can be useful for providing the appropriate strategies and planning of water resources in drought or flood conditions under future increasing temperature.

ACKNOWLEDGMENT

We thank the Iranian Meteorological Organization for providing synoptic meteorological data.

AUTHOR CONTRIBUTIONS

Maryam Mirakbari was involved in methodology, software, and validation; Tayyebeh Mesbahzadeh in conceptualization, investigation, supervision, and writing-original draft; Farshad Soleimani Sardoo in software and Writing-original draft; Mario Marcello Miglietta in writing-review and editing; Nir Krakauer: investigation, writing-review and editing; and Nahid Alipour in data curation, resources, and software.

ORCID

Maryam Mirakbari http://orcid.org/0000-0002-0858-6435
Tayyebeh Mesbahzadeh http://orcid.org/0000-0002-2344-5438

REFERENCES

AghaKouchak, A., Bardossy, A. B., & Habib, E. (2010). Copula-based uncertainty modelling: Application to multisensor precipitation estimates. *Hydrological Processes*, *24*(15), 2111–2124.

Akaike, H. (1974). A new look at the statistical model identification. *IEEE Transactions on Automatic Control*, *19*(6), 716–723.

Alexander, L. V., Zhang, X., Peterson, T. C., Caesar, J., Gleason, B., Klein Tank, A. M. G., ... Vazquez-Aguirre, J. L. (2006). Global observed changes in daily climate extremes of temperature and precipitation. *Journal of Geophysical Research [Atmospheres]*, *111*, D05109.

Almazroui, M., Nazrul Islam, M., Saeed, F., Alkhalaf, A., & Dambul, R. (2017). Assessing the robustness and uncertainties of projected changes in temperature and precipitation in AR5 Global Climate Models over the Arabian Peninsula. *Atmospheric Research*, *194*(2017), 202–213.

Alves, J. M. B., Junior, F. C. V., Chaves, R. R., Silva, E. M., Servain, J., Costa, A. A., ... dosSantos, A. C. S. (2016). Evaluation of the AR4 CMIP3 and the AR5 CMIP5 model and projections for precipitation in Northeast Brazil. *Frontiers in Earth Science*, *4*(44), 1–22.

Amirataee, B., Montaseri, M., & Rezaie, H. (2018). Regional analysis and derivation of copula-based drought Severity-Area-Frequency curve in Lake Urmia basin, Iran. *Journal of Environmental Management*, *206*, 134–144.

Ashraf Vaghefi, S., Keykhai, M., Jahanbakhshi, F., Sheikholeslami, J., Ahmadi, A., Yang, H., & Abbaspour, K. C. (2019). The future of extreme climate in Iran. *Nature*, *9*, 1–11. https://doi.org/10.1038/s41598-018-38071-8

Azam, A., Maeng, S. J., Kim, H. S., & Murtazaev, A. (2018). Copula-based stochastic simulation for regional drought risk assessment in South Korea. *Water*, *10*(4), 1–29.

Battisti, D., & Naylor, R. (2009). Historical warnings of future food insecurity with unprecedented seasonal heat. *Science*, *323*(5911), 240e244. https://doi.org/10.1126/science.1164363.2009

Benth, F. E., & Saltyte-Benth, J. (2005). Stochastic modeling of temperature variations with a view towards weather derivatives. *Applied Mathematical Finance*, *12*(1), 53–85.

Bracken, C., Holman, K. D., Rajagopalan, B., & Moradkhani, H. (2018). A Bayesian hierarchical approach to multivariate nonstationary hydrologic frequency analysis. *Water Resources Research*, *54*(1), 243–255. https://doi.org/10.1002/2017WR020403

Chen, Y. D., Zhang, Q., Xiao, M., Singh, V. P., & Zhang, S. (2016). Probabilistic forecasting of seasonal droughts in the Pearl River basin, China. *Stochastic Environmental Research and Risk Assessment: Research Journal*, *30*, 2031–2040. https://doi.org/10.1007/s00477-015-1174-6

Cheraghalizadeh, M., Ghameshlou, A., Bazrafshan, J., & Bazrafshan, O. (2018). A Copula-based joint meteorological-hydrological drought index in a humid region (Kasilian Basin, North Iran). *Arabian Journal of Geosciences*, *11*(12), 300.

Choi, G., Collins, D., Ren, G., Trewin, B., Baldi, M., Fukuda, Y., ... Zhou, Y. (2009). Changes in means and extreme events of temperature and precipitation in the Asia-Pacific network region, 1955–2007. *International Journal of Climatology*, *29*, 1906–1925.

Cong, R. G., & Brady, M. (2012). The interdependence between rainfall and temperature copula analysis. *Scientific World Journal*, *21*, 1–11.

De Martonne, E. (1925). Traité de Géographie Physique, Vol I: Notions generales, climat, hydrographie. *Geographical Review*, *15*(2), 336–337.

De Michele, C., & Salvadori, G. (2003). A generalized pareto intensity-duration model of storm rainfall exploiting 2-Copulas. *Journal of Geophysical Research*, *108*(D2), 4067. https://doi.org/10.1029/2002JD002534

Dodangeh, E., Shahedi, K., Shiau, J. T., & Mirakbari, M. (2017). Spatial hydrological drought characteristics in Karkheh River basin, southwest Iran using copulas. *Journal Earth System Science*, *126*, 1–20. https://doi.org/10.1007/s12040-017-0863-6

Donat, M. G., Alexander, L. V., Yang, H., Durre, I., Vose, R., Dunn, R. J. H., ... Kitching, S. (2013). Updated analyses of temperature and precipitation extreme indices since the beginning of the twentieth century: The HadEX2 dataset. *Journal of Geophysical Research [Atmospheres]*, *118*, 2098–2118. https://doi.org/10.1002/jgrd.50150

Easterling, D. R., Meehl, G. A., Parmesan, C., Stanley, A., Changnon, T. R. K., & Mearns, L. O. (2000). Climate extremes: Observations, modeling, and impacts. *Science*, *289*, 2068–2074. https://doi.org/10.1126/science.289.5487.2068

Erlat, E., & Türkeş, M. (2013). Observed changes and trends in numbers of summer and tropical days, and the 2010 hot summer in Turkey. *International Journal of Climatology*, *33*, 1898–1908.

Favre, A. C., El Adlouni, S., Thi Emong, N., & Bobee, B. (2004). Multivariate hydrological frequency analysis using copula. *Journal of Water Resources Research*, *40*, 1–12.

Frich, P., Alexander, L. V., Della-Marta, P., Gleason, B., Haylock, M., Klein Tank, A. M. G., & Peterson, T. (2002). Observed coherent changes in climatic extremes during the second half of the twentieth century. *Climate Research*, *19*, 193–212.

Gagnon, S., Singh, B., Rousselle, J., & Roy, L. (2005). An application of the statistical downscaling model (SDSM) to simulate climatic data for stream flow modeling in Québec. *Canadian Water Resources. 30*(4), 297–314.

Genest, C., Favre, A. C., Liveau, B., & Jacques, C. (2007). Metaelliptical copula and their use in frequency analysis of multivariate hydrological data. *Journal of Water Resources Research*, *43*, WR005275.

Gupta, H. V., Kling, H., Yilmaz, K. K., & Martinez, G. F. (2009). Decomposition of the mean squared error and NSE performance criteria: Implications for improving hydrological modeling. *Journal of Hydrology*, *377*(1-2), 80–91.

Graczyk, D., Pińskwar, I., Kundzewicz, Z. W., Hov, O., Forland, E. J., Szwed, M., & Choryński, A. (2017). The heat goes on—Changes in indices of hot extremes in Poland. *Theoretical Applications of Climatology*, *129*, 459–471. https://doi.org/10.1007/s00704-016-1786-x

Grimaldi, S., & Serinaldi, F. (2006). Asymmetric copula in multivariate flood frequency analysis. *Advances in Water Resources*, *29*, 1155–1167. https://doi.org/10.1016/j.advwatres.2005.09.005

Haylock, M. R., Peterson, T. C., Alves, L. M., Ambrizzi, T., Anunciação, Y. M. T., Baez, J., ... Vincent, L. A. (2006). Trends in total and extreme South American rainfall in 1960–2000 and links with sea surface temperature. *Journal of Climate*, *19*, 1490–1512.

IPCC. (1996). *Climate change* (p. 570). Cambridge: Cambridge University Press.

IPCC. (2012). *Managing the risks of extreme events and disasters to advance climate change adaptation*. A Special Report of Working Groups I and II of the Intergovernmental Panel on Climate Change. Cambridge University Press, Cambridge and New York, NY, p. 582.

IPCC (2013). Climate Change (2013): The Physical Science Basis Contribution of Working Group I to the Fifth Assessment Report of the Intergovernmental Panel on Climate Change (p. 1535). Cambridge, United Kingdom and New York, NY: Cambridge University Press.

Jacob, D., Elizalde, A., Haensler, A., Hagemann, S., Kumar, P., Podzun, R., ... Wilhelm, Ch. (2012). Assessing the transferability of the regional climate model REMO to different coordinated regional climate downscaling experiment (CORDEX) regions. *Atmosphere*, *3*, 181–199.

Katz, R. W., & Brown, B. G. (1992). Extreme events in a changing climate: Variability is more important than averages. *Climate Change*, *21*, 289–302. https://doi.org/10.1007/BF00139728

Kendall, M. G. (1975). *Rank correlation methods* (4th ed.). London: Charles Griffin.

Klein Tank, A. M. G., & Können, G. P. (2003). Trends in indices of daily temperature and precipitation extremes in Europe, 1946-99. *Journal of Climate*, *16*, 3665–3680.

Kundzewicz, Z. W., & Huang, S. (2010). Seasonal temperature extremes in Potsdam. *Acta Geophysics*, *58*(6), 1115–1133.

Li, J., Zhang, Q., Chen, Y. D., & Singh, V. P. (2015). Future joint probability behaviors of precipitation extremes across China: Spatiotemporal patterns and implications for flood and drought hazards. *Global and Planetary Change*, *124*, 107–122. https://doi.org/10.1016/j.gloplacha.2014.11.012

Li, R., & Geng, S. (2013). Impacts of climate change on agriculture and adaptive strategies in China. *Integrative Agriculture*, *12*(8), 1402–1408.

Liu, X., Li, N., Yuan, S., Xu, N., Shi, W., & Chen, W. (2015). The joint return period analysis of natural disasters based on monitoring and statistical modeling of multidimensional hazard factors. *Science of the Total Environment*, *538*, 724–732.

Madadgar, Sh, & Moradkhani, H. (2013). Drought analysis under climate change using copula. *Journal of Hydrologic Engineering*, *18*, 746–759.

Mann, H. B. (1945). Nonparametric test against trend. *Journal of Econometrical*, *13*, 245–259.

Mann, M. E., Rahmstorf, S., Kornhuber, K., Steinman, B. A., Miller, S. K., & Coumou, D. (2017). Influence of anthropogenic climate change on planetary wave resonance and extreme weather events. scientific reports. *Nature Publishing Group*, *7*(February), 45242. https://doi.org/10.1038/srep45242

Marengo, J. A., Ambrizzi, T., DaRocha, R. P., Alves, L. M., Cuadra, S. V., Valverde, M. C., ... Ferraz, S. E. T. (2009). Future change of climate in South America in the late twenty-first century: Intercomparison of scenarios from three regional climate models. *Climate Dynamics*, *35*, 1073–1097. https://doi.org/10.1007/s00382-009-0721-6

Meehl, G. A., & Claudia, T. (2004). More intense, more frequent, and longer lasting heat waves in the 21st century. *Science*, *305*, 994–997.

Meehl, G. A., Zwiers, F., Evans, J., & Knutson, T. (2000). Trends in extreme weather and climate events: Issues related to modeling extremes in projections of future climate change. *Bulletin of the American Meteorological Society*, *81*, 427–436.

Mesbahzadeh, T., Miglietta, M. M., Mirakbari, M., Soleimani Sardoo, F., & Abdolhoseini, M. (2019). Joint modeling of precipitation and temperature using copula theory for current and future prediction under climate change scenarios in arid lands (Case Study, Kerman Province, Iran). *Advances in Meteorology*, *2019*, 1–15. https://doi.org/.org/10.1155/2019/6848049

Mirakbari, M., Ganji, A., & Fallah, S. R. (2010). Regional bivariate frequency analysis of meteorological droughts. *Journal of Hydrologic Engineering*, *15*(12), 985–1000.

Moberg, A., & Jones, P. D. (2005). Trends in indices for extremes in daily temperature and precipitation in central and western Europe, 1901–99. *International Journal of Climatology*, *25*, 1149–1171.

Modaresi Rad, A., Ghahraman, B., Khalili, D., Ghahremani, Z., & Ahmadi Ardakani, S. (2017). Integrated meteorological and hydrological drought model: A management tool for proactive water resources planning of semi-arid regions. *Advances in Water Resources*, *107*, 336–353.

Nasri, M., & Modarres, R. (2009). Dry spell trend analysis of Isfahan Province, Iran. *International Journal of Climatology*, *29*, 1430–1438.

Nelsen, R. B. (2006). *An introduction to copulas*. New York, NY: Springer.

Nemec, J., Gruber, C., Chimani, B., & Auer, I. (2013). Trends in extreme temperature indices in Austria based on a new homogenized dataset. *International Journal of Climatology*, *33*, 1538–1550.

Ngo, N. S., & Horton, R. M. (2016). Climate change and fetal health: The impacts of exposure to extreme temperatures in New York City. *Environmental Research*, *144*, 158–164.

Onoz, B., & Bayazit, M. (2003). The power of statistical tests for trend detection. *Turkish Journal of Engineering Environmental Science*, *27*, 247–251.

Palatella, L., Miglietta, M. M., Paradisi, P., & Lionello, P. (2010). Climate change assessment for Mediterranean agricultural areas by statistical downscaling. *Natural Hazards and Earth System Sciences*, *10*, 1647–1661. https://doi.org/10.5194/nhess-10-1647-2010

Pandey, P., Das, L., Jhajharia, D., & Pandey, V. (2018). Modeling of interdependence between rainfall and temperature using copula. *Modeling Earth Systems and Environment*, *4*(2), 867–879.

Pervez, M. S., & Henebry, G. F. (2014). Projections of the Ganges–Brahmaputra precipitation—Downscaled from GCM predictors. *Journal of Hydrology*, *517*, 120–134.

Pietikäinen, J. P., Markkanen, T., Sieck, K., Jacob, D., Korhonen, J., Räisänen, P., ... Kau, J. (2018). The regional climate model REMO (v2015) coupled with the 1-D freshwater lake model FLake (v1): Fenno-Scandinavian climate and lakes. *Geoscientific Model Development*, *11*(4), 1321–1342. https://doi.org/10.5194/gmd-11-1321-2018

Sajjad, H., & Ghaffar, A. (2018). Observed, simulated and projected extreme climate indices over Pakistan in changing climate. *Theoretical and Applied Climatology*, *137*, 255–281. https://doi.org/10.1007/s00704-018-2573-7

Salvadori, G., & De Michele, C. (2004). Frequency analysis via Copulas: Theoretical aspects and applications to hydrological events. *Water Resources Research*, *40*, 5546. https://doi.org/10.1029/2004WR003133

Santos, C. A. C., & Oliveira, V. G. (2017). Trends in extreme climate indices for Pará State, Brazil. *Revista Brasileira de Meteorologia*, *32*(1), 13–24.

Shiau, J. T. (2006). Fitting drought duration and severity with two-dimensional copulas. *Water Resources Management*, *20*(5), 795–815.

Sillmann, J., Kharin, V. V., Zwiers, F. W., Zhang, X., & Bronaugh, D. (2013). Climate extremes indices in the CMIP5 multimodel ensemble: Part 2. Future climate projections. *Journal of Geophysical Research [Atmospheres]*, *118*, 2473–2493.

Sillmann, J., & Roeckner, E. (2008). Indices for extreme events in projections of anthropogenic climate change. *Climate Change*, *86*, 83–104.

Silva, G. A., & Mendes, D. (2015). Refinement of the daily precipitation simulated by the CMIP5 models over the north of the Northeast of Brazil. *Frontiers of Environmental Science*, *3*, 29. https://doi.org/10.3389/fenvs.2015.00029

Sisco, M. R., Bosetti, V., & Weber, E. U. (2017). When do extreme weather events generate attention to climate change? *Climatic Change*, *143*(1–2), 227–241. https://doi.org/10.1007/s10584-017-1984-2

Sklar, A. (1959). Fonctions der 'epartition' an dimensionset leursmarges. *Publications de l'Institut de Statistique de l'Universit´e de Paris*, *8*, 229–231.

Tebaldi, C., Hayhoe, K., Arblaster, J. M., & Meehl, G. A. (2006). Going to the extremes. *Climate Change*, *79*, 185–211.

Thomson, A. M., Calvin, K. V., Smith, S. J., Page Kyle, G., Volke, A., Patel, P., ... Edmonds, J. A. (2011). RCP4.5: A pathway for stabilization of radiative forcing by 2100. *Climatic Change*, *109*(1-2), 77–94. https://doi.org/10.1007/s10584-011-0151-4

Ujeneza, E. L. (2014). Simulation the Characteristics of Droughts in Southern Africa. *MSc thesis, University of Cape Town*.

Uttam, P., Goswami, U. P., Bhargav, K., Hazra, B., & Goyal, M. K. (2018). Spatiotemporal and joint probability behavior of temperature extremes over the Himalayan region under changing climate. *Theoretical and Applied Climatology*, *134*, 1–22. https://doi.org/10.1007/s00704-017-2288-1

Vogt, D. J., Vogt, K. A., Gmur, S. J., Scullion, J. J., Suntana, A. S., Daryanto, S., & Sigurðardóttir, R. (2016). Vulnerability of tropical forest ecosystems and forest dependent communities to droughts. *Environmental Research*, *144*, 27–38.

Wang, X., Gebremichael, M., & Yan, J. (2010). Weighted likelihood copula modeling of extreme rainfall events in Connecticut. *Journal of Hydrology*, *390*, 108–115. https://doi.org/10.1016/j.jhydrol.2010.06.039

WMO. (2013). *The global climate 2001–2010: A decade of climate extremes–summary report* (WMO no.1119). Author, Geneva, Switzerland (20pp).

Zhang, L., & Singh, V. P. (2007). Bivariate rainfall frequency distributions using Archimedean copulas. *Journal of Hydrology*, *332*, 93–109. https://doi.org/10.1016/j.jhydrol.2006.06.033

Zhang, Q., Li, J., Singh, V. P., & Xu, C. Y. (2013). Copula-based spatial-temporal patterns of precipitation extremes in China. *International Journal of Climatology*, *33*, 1140–1152. https://doi.org/10.1002/joc.3499

Zhang, X., Hegerl, G., Zwiers, F. W., & Kenyon, J. (2005b). Avoiding in homogeneity in percentile-based indices of temperature extremes. *Journal of Climate*, *18*, 1641–1651.

Zhang, X., & Yang, F. RClimDex (1.0) User Guide. Climate Research Branch Environment Canada: Downsview, Ontario, Canada, 2004.

How to cite this article: Mirakbari M, Mesbahzadeh T, Soleimani Sardoo F, Miglietta MM, Krakauer NY, Alipour N. Observed and projected trends of extreme precipitation and maximum temperature during 1992–2100 in Isfahan province, Iran using REMO model and copula theory. *Natural Resource Modeling*. 2020;33:e12254. https://doi.org/10.1111/nrm.12254